Kinetic arrest, dynamical transitions, and activated relaxation in dense fluids of attractive nonspherical colloids

Rui Zhang and Kenneth S. Schweizer

Phys. Rev. E **83**, 060502 — Published 28 June 2011

DOI: 10.1103/PhysRevE.83.060502

Physical Review Letters, submitted, March, 2011
Revised and resubmitted as a Rapid Communication to PRE, May, 2011; Accepted

Kinetic Arrest, Dynamical Transitions, and Activated Relaxation in Dense Fluids of Attractive Nonspherical Colloids

Rui Zhang and Kenneth S. Schweizer*

Department of Materials Science and Frederick Seitz Materials Research Laboratory,

University of Illinois, 1304 West Green Street, Urbana, lllinois 61801, USA

*kschweiz@illinois.edu

PACS numbers: 64.70.Q-, 82.70.Dd, 83.80.Hj

Abstract

The coupled translation-rotation activated dynamics in dense suspensions of attractive homogeneous and Janus uniaxial dicolloids are studied using microscopic statistical mechanical theory. Multiple kinetic arrest transitions and re-entrant phenomena are predicted associated with fluid, gel, repulsive glass, attractive glass, plastic glass, and novel glass-gel states. The activated relaxation rate is a nonuniversal non-monotonic function of attraction strength at high volume fractions due to the consequences of a change of transient localization mechanism from caging to physical bonding.

The field of colloid and nanoparticle science is presently undergoing rapid expansion in the new direction of dense suspensions composed of nonspherical and/or chemically heterogeneous (e.g., Janus) particles of modest shape anisotropy, objects sometimes called "colloidal molecules" [1,2]. Nonsphericity introduces the qualitatively new effect of coupled translation-rotation motion which can result in distinctive slow dynamics, viscoelasticity and kinetically arrested states. For hard core uniaxial particles, ideal mode coupling theory (MCT) [3-5], the activated barrier hopping nonlinear Langevin equation (NLE) theory [5-7], and simulations [8] have established that modest shape anisotropy can result in the emergence of plastic glasses (liquid-like rotations, localized translations) and double glasses (localized translation and rotation). Moreover, particle nonsphericity can either promote or suppress kinetic arrest depending on the degree of shape anisotropy, and intriguing connections with the jamming of granular ellipsoids and spherocylinders have been found [9,10]. Very recent measurements of kinetic arrest and elasticity in suspensions of repulsive nonspherical dicolloids and tricolloids have been performed [10] which support the microscopic MCT and NLE theories. Also, two-step nonlinear yielding (stress-driven solid-to-liquid transition) has been discovered for glassy dicolloid suspensions which has been interpreted as sequential unlocking of orientational and translational dynamical constraints [11].

In contrast to the significant recent theoretical progress for repulsive uniaxial particles, the question of how short range attractions modify slow dynamics is untouched. Given the rich behavior of spheres that interact via short range attractions, including phenomena such as [12-17] the emergence of gels and attractive glasses, a re-entrant glass-fluid-gel transition, non-monotonic diffusivity as a function of attraction strength,

and two-step yielding, one suspects new dynamical phenomena await discovery for dense suspensions of nonspherical colloids. The purpose of this Rapid Communication is to present the first theoretical study of the onset of slow dynamics and strongly activated relaxation in dense suspensions of sticky homogeneous and Janus dicolloids. We address the following open questions: (1) how do attractions modify the fluid (F) → plastic glass (PG) → double glass transition with increasing volume fraction for low aspect ratio dicolloids ? (2) How does particle shape anisotropy modify the repulsive glass (RG) → F →gel (G) re-entrant transition ? (3) What is the nature of the localized and activated transition states in attractive glasses (AG) ? (4) Can activated relaxation and diffusion vary non-monotonically with attraction strength ? (5) At the dynamic crossover level, do new arrested states emerge ? (6) How does chemical heterogeneity and clustering in Janus dicolloid fluids modify slow dynamics ?

We study the above questions using naïve MCT (NMCT) and the NLE theory of activated barrier hopping for uniaxial particles [6]. The conceptual basis and detailed equations of these approaches are well documented [6]. Structural correlations are determined based on an interaction site model and the Reference Interaction Site Model (RISM) integral equation theory [18]. NLE theory describes single particle dynamics via 2 coupled stochastic equations-of-motion for the center-of-mass displacement (CM) and cumulative rotational angle dynamical variables (both zero at t=0) which in the overdamped limit are [6]:

$$\zeta_T \frac{d}{dt} r_{CM}(t) = -\frac{\partial}{\partial r_{CM}} F_{eff}(r_{CM}, \theta) + \delta f_T(t) \qquad (1)$$

$$\zeta_R \frac{d}{dt} \theta(t) = -\frac{\partial}{\partial \theta} F_{eff}(r_{CM}, \theta) + \delta T_R(t) \qquad (2)$$

The key object is the 2-dimensional dynamic free energy surface, F_{eff}, which self-consistently quantifies the force and torque on a tagged particle due to its surroundings, and can be a priori computed from knowledge of equilibrium structure (site-site direct correlation functions and structure factors). The quantities δf_T and δT_R describe the white noise random force and torque, respectively, and ζ_T and ζ_R are short-time translational and rotational friction constants, respectively. Dropping the noise terms in Eqs(1) and (2) yields the NMCT self-consistency equations for the long time mean square value of the two dynamic order parameters. The first emergence of non-infinite values of the latter defines an ideal kinetic arrest transition which signals a dynamic crossover to activated relaxation. Multi-dimensional Kramers theory allows computation of the mean first passage time over the saddle point transition state barrier of the dynamic free energy [6].

Our theory can be used to study dicolloids of any aspect ratio, and different levels of attractions between the 2-sites of the particle; the role of aspect ratio has been thoroughly established in the context of hard core dicolloids [6]. Here, we choose to study three specific two-site particle systems that best elucidate the key new physics representative of the wide parameter space that characterizes this class of particles. Homogeneous dicolloids (hDC) of aspect ratio L/D = 1.3 and 2 where each site (diameter, D) interacts via a hard core repulsion plus an attractive exponential tail of range a=0.02D of variable contact strength, ε (in thermal energy units), and a L/D = 2 maximally frustrated Janus dicolloid (JDC) composed of one attractive and one hard core site. The repulsive L/D=1.3 system is representative of low aspect ratio particles (and has been studied experimentally [10]) that exhibit a plastic glass state over a high volume fraction interval under hard core

conditions [4,6]. In contrast, the L/D=2 dicolloid is representative of the higher aspect ratio particles which exhibit strongly coupled translation-rotation activated dynamics and only a "double glass" ideal localization transition [4-6]. The Janus dicolloid is the extreme member of a family of chemically heterogeneous (or "patchy") attractive particles. Hence, it is expected to exhibit the most dramatic differences compared to its chemically homogeneous analog, and such Janus colloids are of intense experimental interest [2].

Figure 1 presents the NMCT kinetic arrest map for the two L/D=2 dicolloids. The homogeneous system exhibits : fluid, repulsive glass, attractive glass, and gel states, a re-entrant RG→F→AG transition region upon increasing attraction strength at high volume fraction, and a RG→AG transition beyond the cusp-like "nose" feature at $\varepsilon \sim$ 2.2 which terminates at a "A3" point in MCT language. While the Janus particle shows the same type of kinetically arrested states, there are major quantitative differences: (i) the re-entrant region is essentially destroyed which we can understand as the consequence of the fact that we predict the reduction of short range order (as quantified by the static structure factor cage peak) for weak attractions in the re-entrant hDC system does not occur for Janus particles, and (ii) the nose feature and gel line occur at significantly higher attraction strengths. Points (i) and (ii) are related to the distinct packing structure of the Janus particle fluid, i.e., compact clustering of attractive sites or local self-assembly as indicated by (not shown) the emergence of a "pre-peak" in the sticky-sticky site (s-s) partial structure factor at a wave vector $kD \sim 2.5$ (far below the wide angle cage peak) and an enormous growth of the s-s pair correlation function near contact that far exceeds its hDC analog. A third major difference is the RG→AG boundary is

much broader for the Janus dicolloid compared to the hDC system. The inset shows the CM localization length and angle along the ideal nonergodicity boundary abruptly changes from glass-like to gel-like localization.

The ideal kinetic arrest map for the L/D=1.3 dicolloid is shown in Fig. 2, and exhibits multiple new interesting features. In addition to the F→ PG → RG transition under hard core conditions, there are six other "transitions" (dynamic crossovers) evident based on either a vertical (PG→F→G re-entrant; RG→PG→AG re-entrant; RG→AG (dashed curve); F→G at lower volume fraction) or a horizontal (F→PG→AG; F→G) trajectory in the kinetic arrest map. Moreover, a "dynamic triple point" occurs near ϕ~0.55 and ε~2.1 where the G, F and PG states merge signaling the disappearance of the plastic glass for strong attractions (physical bonding). A qualitatively new kinetically localized state emerges below the nose region along the PG-RG boundary at ε~1.25. Its character is revealed in the inset and corresponds to jumps of the CM and rotational localization parameters from (high) glass-like values to smaller intermediate values. However, the latter are much larger than the very small values characteristic of the gel or attractive glass states. We thus call this intermediate attraction strength kinetically arrested state a "glass-gel" (GG), and note the change of the CM localization length is significantly less its rotational analog. The top inset shows the RG→AG (dashed) curve beyond the "nose", corresponding to a discontinuous jump of the localization length from glass-like to gel-like, is very narrow in breadth for the L/D=1.3 dicolloids. Hence, the extent of this feature is predicted to be very sensitive to particle aspect ratio.

We now numerically study the dynamic free energy surface beyond the ideal NMCT boundaries, and discuss its key features: the coordinates of the localization well and

saddle point barrier, and barrier height. These properties determine the physical character of the stochastic trajectories required to escape the confining effects of the repulsive (caging) and attractive (bond formation) forces, and allow computation of the mean first barrier passage time using multi-dimensional Kramers theory [6]. The latter is a qualitative surrogate for transport properties such as the inverse self-diffusion constant.

Figure 3 present calculations of the mean hopping time (relative to its limiting hard core value) as a function of ε for the L/D=2 hDC at four volume fractions beyond the nose feature in Fig.1. The lowest volume fraction (ϕ=0.5) trajectory goes through the A3 point. In all cases, the relaxation time is a striking non-monotonic function of attraction strength. The relaxation rate enhancement varies from a factor of ~ 5 to 30; it is systematically weaker, occurs at a lower attraction strength, and becomes less abrupt as volume fraction grows. As confirmed by our structure calculations, these trends reflect the relatively larger importance of repulsive forces, which inhibit attraction driven local structure changes, as the fluid densifies. An AG state is eventually always realized at high enough ε where physical bonding results in an increasingly high barrier and upswing of the relaxation time. Qualitatively, such non-monotonic behavior (of comparable amplitude) has been experimentally observed for the diffusion constant in dense spherical particle suspensions [16], and also in simulation [17].

The inset of Fig. 3 presents a representative comparison of the two hDC and Janus particle systems where the volume fractions for each system are chosen to keep fixed the distance from the nose feature in their dynamic crossover diagram. The Janus system behaves significantly differently than the hDC systems, and the more anisotropic L/D=2 hDC system exhibits a modestly larger speeding up of relaxation compared to its

L/D=1.3 analog. Note that since the origin of the non-monotonic relaxation involves activated (not precursor MCT) dynamics, the highly variable breadth of the RG→AG ideal NMCT boundary for the L/D=1.3 and 2 systems is not a crucial feature.

How can one physically understand the results in Figure 3 ? The key is to examine the nature of reactive trajectories over the saddle point as a function of particle anisotropy and attraction strength. Figure 4 presents an example dynamic free energy surface, indicating the coordinates of the localization well and saddle point. The inset plots saddle trajectory cuts projected along the rotational angle coordinate (projections along the CM direction are qualitatively identical). Results are shown at four locations in the dynamic arrest diagram: three fixed volume fraction states (ϕ=0.52) at attraction strengths indicated in Fig.3 by the square (athermal, ε=0), triangle (minimum relaxation time state), and cross (attractive glass with the same relaxation time as the athermal hard core state), plus a gel-like state at lower ϕ but even higher ε.

The athermal system in Fig.4 exhibits a relatively large localization angle and barrier location characteristic of a repulsive (caging controlled) glass. As attractions increase and the relaxation time attains a minimum, both the height and (glass-like) location of the barrier remain essentially unchanged. Hence, the relaxation time non-monotonicity is not a consequence of variation of the activated barrier height, as one might have guessed. Rather, the origin of relaxation acceleration is a large reduction of the localization angle to a gel-like value consistent with the emergence of the AG state. A crucial consequence is the local curvature of localization well increases dramatically, which thereby greatly increases the attempt frequency to surmount the barrier, resulting in a large reduction of the kinetic prefactor in the mean hopping time. As attractions further increase, the

localization well remains largely unchanged, but the barrier height grows significantly since motion now requires cage escape and breakage of physical bonds well in excess of thermal energy, resulting in the strong upswing of the relaxation time at large ε.

Two additional interesting features are illustrated in the upper inset of Figure 4. First, since both AG states exhibit gel-like localization but a glass-like barrier displacement, the relaxation process is expected to be of a "two-step" nature corresponding to first breaking bonds followed by cage escape. This scenario is qualitatively consistent with a recent simulation study of the single particle mean square displacement in dense fluids of attractive spheres [13]. Second, note the AG state differs from the gel not in terms of the localized state which is controlled by tight physical bonding, but rather by the much larger (glass-like) degree of rotation required to surmount the activation barrier in the AG state. This difference in the transition state implies activated stochastic trajectories will exhibit measurable differences in the G and AG states, a prediction that is testable via confocal microscopy.

We have performed many other calculations that buttress the above physical picture that cannot be shown due to space limitations. For example, for the L/D=2 systems at high attraction strength (e.g., ε~3-4) the rotation localization angle is very small since it is controlled by physical bonding. However, the transition state (barrier location) qualitatively changes from gel-like to glass-like with increasing volume fraction (G→AG crossover); an example is shown in lower inset of Fig.4 where the smooth, but well defined, crossover occurs at ϕ~0.48. At a fixed volume fraction beyond the nose feature, with increasing ε the re-entrant effect is predicted where weak attractions initially loosen

transient localization in the RG, before they dominate resulting in massive reduction of vibrational and librational amplitudes in the AG.

In conclusion, we have presented the first theoretical study of coupled translation-rotation activated dynamics in dense suspensions of attractive dicolloids, both homogeneous and Janus, which answers the six questions posed in the Introduction. The new dynamical phenomena discovered are representative of the behavior of the wide class of variable aspect ratio nonspherical particles composed of two interaction sites that experience different degrees of attraction. Our predictions are amenable to testing via simulations, and diffusion, relaxation and confocal microscopy experiments. The present study sets the stage for developing a theory of stress-driven melting of repulsive and attractive glasses, gels, and plastic glasses in dicolloid suspensions, including the puzzling observation of two-step yielding under repulsive interaction conditions [11].

Acknowledgements. This work was supported by DOE-BES via grant number DE-FG02-07ER46471 administered through the Seitz Materials Research Laboratory.

References

[1] S.C.Glotzer and M.J.Solomon, Nature Mater. **6**, 557 (2007); A. van Blaaderen, Nature **439**, 545 (2006).

[2] S.Jiang, Q.Chen, M.Tripathy, E.Luijten, K.S.Schweizer and S.Granick, Adv.Mater. **22**, 1060 (2010).

[3] M.Letz, R.Schilling and A.Latz, Phys.Rev.E **62**, 5173 (2000).

[4] S.H.Chong and W.Götze, Phys.Rev.E **65**, 041503 and 051201 (2002)

[5] G.Yatsenko and K.S.Schweizer, Phys.Rev.E **76**, 041506 (2007).

[6] R.Zhang and K.S.Schweizer, Phys.Rev.E **80**, 011502 (2009); J.Chem.Phys. **133**, 104902 (2010).

[7] K.S.Schweizer and E.J.Saltzman, J.Chem.Phys. **119**, 1181 (2003); K.S.Schweizer,

ibid, **123**, 244501(2005).
[8] A.J.Moreno, S.-H.Chong, W.Kob and F.Sciortino, J.Chem.Phys. **123**, 204505 (2005); C.DeMichele, R.Schilling and F. Sciortino, Phys.Rev.Lett. **98**, 265702(2007).
[9] A.Donev, I.Cisse, D.Sachs, E.A.Variano, F.H.Stillinger, R.Connelly, S.Torquato, and P.M.Chaikin, Science **303**, 990 (2004); S.R.Williams and A.P.Philipse, Phys.Rev.E **67**, 051301 (2003).
[10] R.C.Kramb, R.Zhang, K.S.Schweizer and C.F.Zukoski, Phys.Rev.Lett. **105**, 055702 (2010); J.Chem.Phys. **134**, 014502 (2011).
[11] R.Kramb and C.F.Zukoski, J.Phys.Condens.Matter **23**, 035102 (2011).
[12] F.Sciortino, Nature Mater., **1**, 145 (2002); K.A.Dawson, Curr.Opin.Colloid Interface Sci. **7**, 2187 (2002).
[13] E.Zaccarelli and W.C.K.Poon, Proc.Natl.Acad.Sci. **106**, 15203 (2009).
[14] K.N.Pham, A.M.Puertas, J.Bergenholtz, S.U.Egelhaaf, A.Moussaïd, P.N.Pusey, A.B. Schofield, M.E.Cates, M.Fuchs, and W.C.K. Poon, Science **296**, 104 (2002).
[15] A.Latka, Y.Han, A.M.Alsayed, A.B.Schofield, A.G.Yodh and P. Habdas, Europhys. Lett. **86**, 58001 (2009); L.J.Kaufman and D.A.Weitz, J.Chem.Phys. **125**, 074716 (2006).
[16] D.R.Reichman, E.Rabani, and P.L.Geissler, J.Phys.Chem.B **109**, 14654 (2005).
[17] K.N.Pham, G.Petekidis, D.Vlassopoulos, S.U.Egelhaaf, W.C.K.Poon and P.N.Pusey, J.Rheology **52**, 649 (2008).
[18] D.Chandler and H.C.Andersen, J.Chem.Phys. **57**, 1930 (1972).

Figure Captions

FIG.1 (Color online) NMCT kinetic arrest diagrams in the representation of contact attraction strength versus volume fraction for L/D=2 hDC and JDC systems. Curves represent ideal nonergodicity (dynamic crossover) boundaries at which the localization length and angle simultaneously undergo a discontinuous transition. Inset: localization length and angle (dashed curves) as a function of attraction strength along the ideal arrest boundaries.

FIG.2 (Color online) NMCT kinetic arrest diagrams for the L/D=1.3 hDC system. Two ideal nonergodicity boundaries represent the fluid-plastic glass transition (blue square) and double localization transition (green star).Left inset: localization length and angle (dashed curves) as a function of attraction strength along the double localization boundary. Upper inset: enlarged view of the nose region showing the narrow RG→AG boundary.

FIG.3. (Color online) Dimensionless mean barrier hopping time (normalized by its limiting value under purely repulsive conditions) as a function of attraction strength for the L/D=2 hDC at four volume fractions. Inset: comparison of the dimensionless mean hopping time for the three types of particles at fixed $\phi - \phi_{nose} = 0.075$.

FIG.4. (Color online) Dynamic free-energy surface as a function of CM and rotational angle displacements for the L/D=2 hDC system at $\phi = 0.52, \varepsilon = 2.4$. The two shaded dots indicate the localized state and saddle point. Upper inset: 1-d cuts along the saddle reaction trajectory as a function of rotational angle displacement for the three states ($\phi = 0.52$) labeled in Fig.3 by the large black square, triangle and cross, and a gel state ($\phi = 0.35, \varepsilon = 4$). Lower inset: rotational angle displacement in the localized state (lower curve) and at the saddle point (upper curve) as a function of volume fraction for $\varepsilon = 3$.

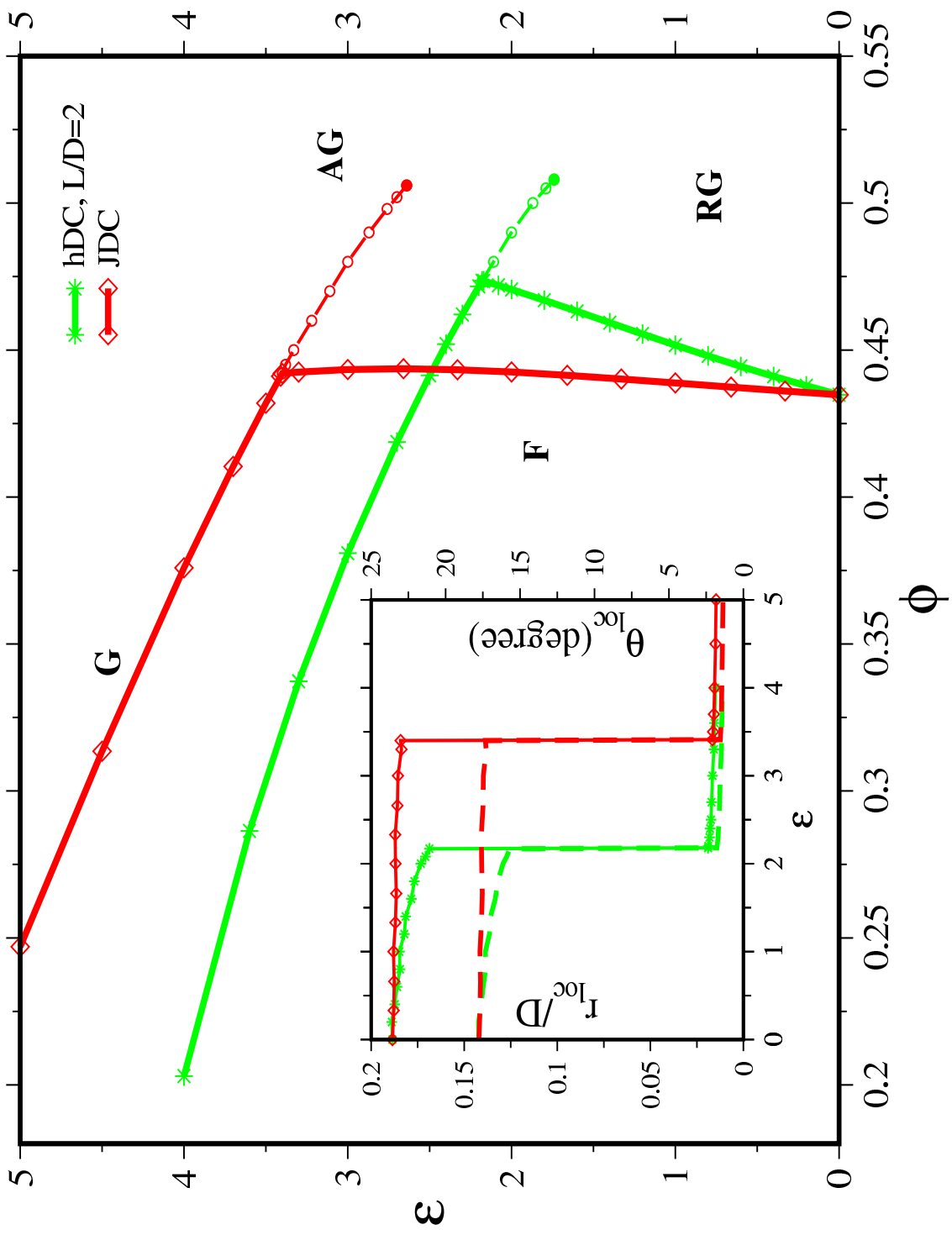

Figure 1 LC13450ER 27MAY2011

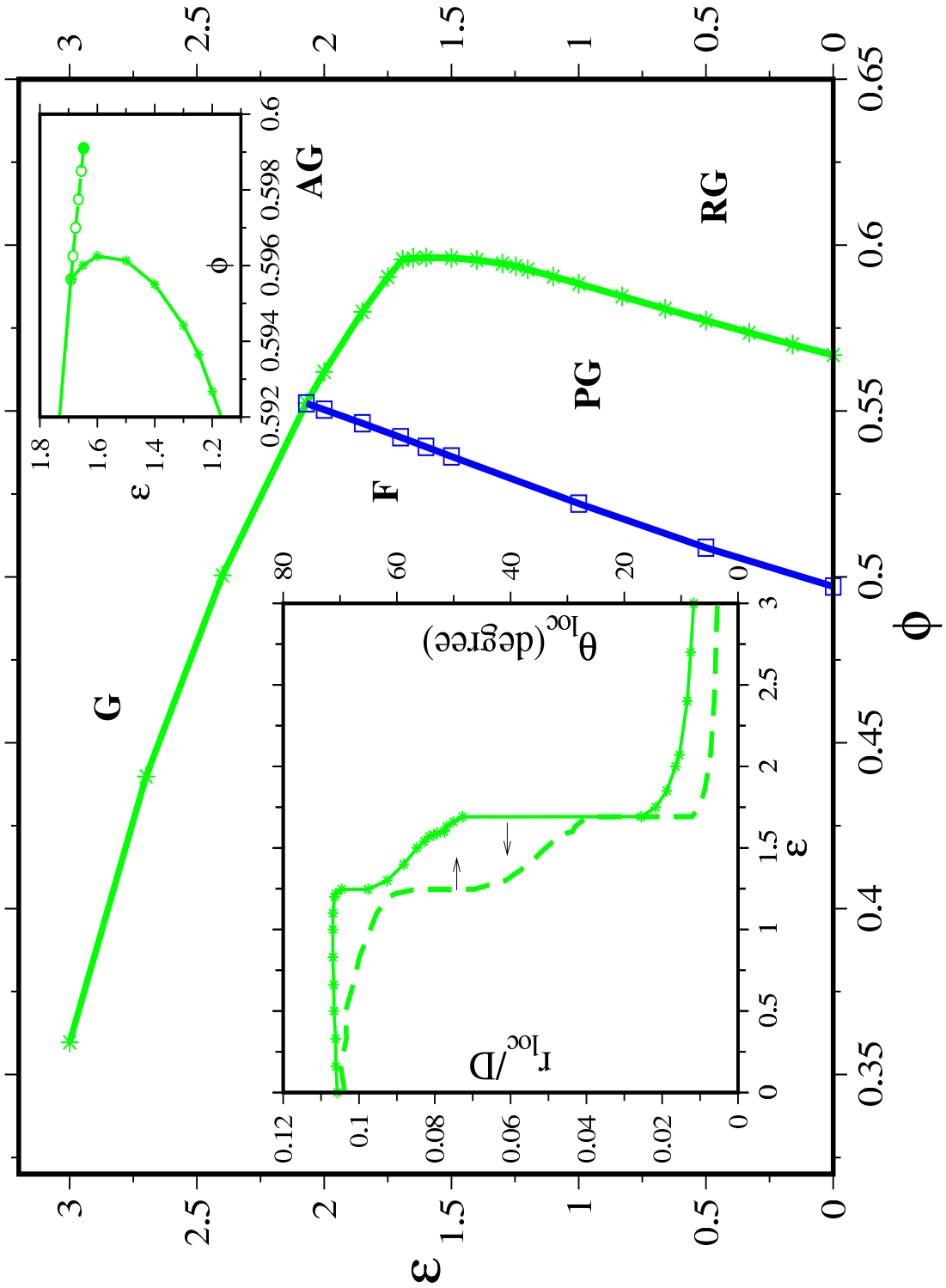

Figure 2 LC13450ER 27MAY2011

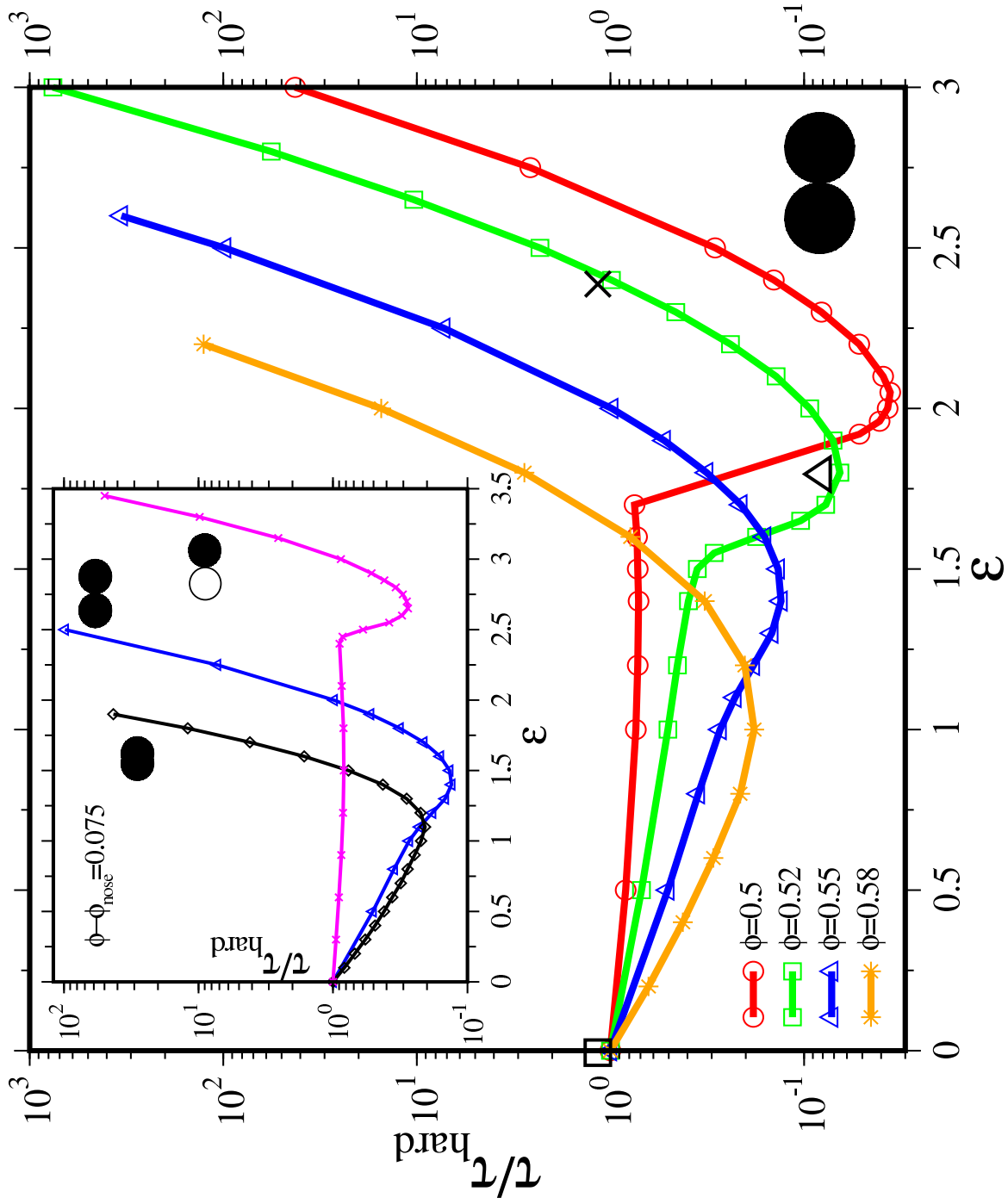

Figure 3 LC13450ER 27MAY2011

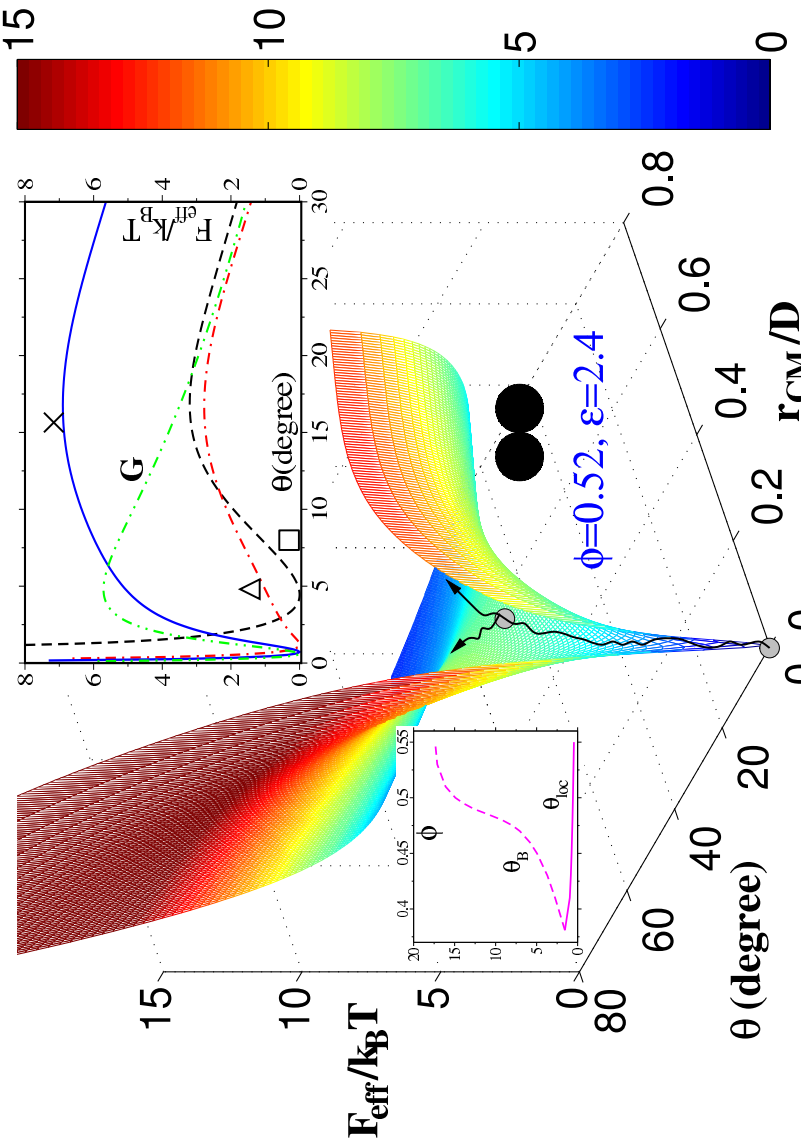

Figure 4 LC13450ER 27MAY2011